J. Iran. Chem. Soc., Vol. 7, Suppl., July 2010, pp. S130-S144.

JOURNAL OF THE
Iranian
Chemical Society

Cetyltrimethylammonium Bromide-Coated Magnetite Nanoparticles as Highly Efficient Adsorbent for Rapid Removal of Reactive Dyes from the Textile Companies' Wastewaters

M. Faraji[a], Y. Yamini[a,*], E. Tahmasebi[a], A. Saleh[a] and F. Nourmohammadian[b]
[a]*Department of Chemistry, Tarbiat Modares University, P.O. Box 14115-175, Tehran, Iran*
[b]*Department of Colorant Manufacture, Iran Color Research Center, Tehran, Iran*

(Received 12 December 2009, Accepted 25 February 2010)

The utilization of modified magnetite nanoparticles (Fe_3O_4 NPs) with a cationic surfactant (cetyltrimethylammonium bromide (CTAB)) as an efficient adsorbent was successfully carried out to remove reactive black 5 (RBBA), reactive red 198 (RRR) and reactive blue 21 (RTB) dyes from aqueous solutions. First, a reactor was designed to be simple, repeatable and efficient in its synthesis of Fe_3O_4 NPs via co-precipitation method. Then, an orthogonal array design (OAD), four factor-four level (4^4) matrix was applied to assign affecting factors on removing of the dyes from aqueous solutions. The obtained results from ANOVA showed that the amount of CTAB and NaCl% significantly affect the adsorption of RBBA, RRR and RTB dyes. The sorption kinetics of the dyes were best described by a second-order kinetic model, suggesting chemisorptions mechanism. Also, dye adsorption equilibrium state data were fitted well to the Langmuir isotherm rather than Freundlich isotherm. Also, the maximum monolayer capacity, q_{max}, obtained from the Langmuir was 312.5, 163.9 and 556.2 mg g^{-1} for RBBA, RRR and RTB, respectively. The obtained results in the present study indicated that the CTAB-coated Fe_3O_4 NPs can be an efficient adsorbent material for removal of reactive dyes form aqueous solutions.

Keywords: Magnetite nanoparticles, Reactive dyes, Removal, Orthogonal array design

INTRODUCTION

The treatment of wastewater has long been a major concern to environmentalists. Dye pollutants in our wastewaters, are a major source of environmental contamination. The total amount of dye consumption by the textile industries worldwide is in the excess of 10^7 kg per year. Approximately one million kilograms of dyes are discharged per year into our waters and streams by the textile industries [1].

Reactive dyes are extensively used in the textile industry, fundamentally due to their ability in their reactive groups to binding onto the textile fibers through covalent bonds [2]. The major environmental problem associated with the use of reactive dyes is their loss in the dyeing process since the fixation efficiency ranges from 60 to 90% [3]. Consequently, substantial amounts of unfixed dyes which are then released into the wastewaters display high organic loads. These pollutants are indicated by the high chemical oxygen demand (COD), low biodegradability and high-salt content in the textile wastewaters. Therefore, for treatment of dye-containing effluents different techniques have been used up to date [4]. Among the techniques, adsorption technique offers significant advantages over the other removal techniques. The adsorption technique is more economical, simpler [5], and is capable to

*Corresponding author. E-mail: yyamini@modares.ac.ir

efficiently treat dyes in their more concentrated forms [6]. Also, adsorption techniques don't have secondary sludge disposal problems, making it environmental friendly [7]. Although, activated carbon is widely used as an efficient adsorbent for dye removal from colored waters owing to its excellent adsorption abilities, it suffers from several drawbacks such as its high price both to the manufacturer and it is also ineffective against dispersing and vat dye [8]. Hence, the alternative low-cost, novel locally, and the availability of adsorbents is currently the motivation behind the removal of textile dye effluents from aqueous solutions, instead of activated carbon. Sepiolite [9], zeolite [10], waste metal hydroxide sludge [11], smectite [12], bentonite [13], Sorrel's cement [14], modified mesoporous silica [15], orange peel [16], polymethylacrylate grafted chitosan [17], sunflower seed shells [8], magnetic alginate beads [18] and modified magnetic nanoparticles [19, 20] are some adsorbents that have been used in this respect.

Recently, nanometer-sized materials have attracted substantial interest in the scientific community because of their special properties [21]. These materials have been used in various scientific fields such as biotechnology, engineering, biomedical, environmental, and material science [22-26]. The application of NPs as SPE adsorbents for pollutant removal is gaining the researcher's interest [26-31]. Compared with micrometer-sized particles, NPs offers a significantly higher surface area-to-volume ratio and a short diffusion route, resulting in high extraction capacity, rapid extraction dynamics and high extraction efficiencies [32]. Superparamagnetic NPs such as Fe_3O_4, are attracted to a magnetic field but retain no residual magnetism after the field has been removed. This property makes them particularly suitable for pollutant removal because no centrifugation or filtrations (versus non-magnetic NPs) of the sample are then needed.

The aim of the present work is to investigate the removal of three reactive dyes; reactive black 5 (RBBA), reactive red 198 (RRR) and reactive blue 21 (RTB) from colored wastewaters by adsorption onto cetyltrimethylammonium bromide coated magnetite NPs (CTAB-coated Fe_3O_4 NPs). For this purpose, first design of a systematic synthesis procedure for simple, repeatable and large scale production of Fe_3O_4 NPs will be investigated. In continue affecting parameters on the adsorption of the dyes, kinetic and isotherm of the dyes adsorption will be discussed.

EXPERIMENTAL

Chemical and Apparatus

All reagents were of analytical reagent grade and were used as supplied. RBBA, RRR and RTB were obtained from Dystar (Frankfurt, Germany). Ferric chloride ($FeCl_3.6H_2O$), ferrous chloride ($FeCl_2.4H_2O$), sodium hydroxide, cetyltrimethylammonium bromide (CTAB), methanol, acetone, sodium carbonate, sodium sulfate, and hydrochloric acid were prepared from Merck (Darmstadt, Germany). Double distilled water was used throughout the experiments. The dyes stock solutions were prepared in the double distilled water.

All of spectrophotometric measurements of the reactive dyes were done at their λ_{max} (580, 514 and 500 nm for RBBA, RRR and RTB, respectively) by a Cesil CE-7200 UV-Vis spectrophotometer (Cambridge, England). Molecular structures of the dyes are shown in Fig. 1. The pHs of solutions were measured with a WTW Inolab (Weilheim, Germany) pH meter supplied with a combined electrode. Magnetic separation was done by a strong magnet with 1.4 Tesla magnetic fields (10 × 5 × 4 cm). A Heidolph motor-stirrer (Schwabach, Germany) was applied for stirring of the dye solutions with a glassware stirrer. A shaker with a temperature controller was applied for shaking of the dye solutions in the isotherm studies at a constant temperature. X-ray powder diffraction (XRD) measurements were performed using a Philips diffractometer of X'pert Company with mono chromatized Cu k_α radiation. The samples were characterized with a scanning electron microscope (SEM) (Philips XL30, Eindhoven, The Netherlands with gold coating. The information of the Infra red (IR) spectra was recorded on a Shimadzu–IR460 spectrometer in a KBr matrix.

Reactor Design to NPs Synthesis

In order to simple, repeatable and large scale synthesis of Fe_3O_4 NPs with high efficiency which is a primer request for removal of large amounts of dyes from wastewaters, a five-

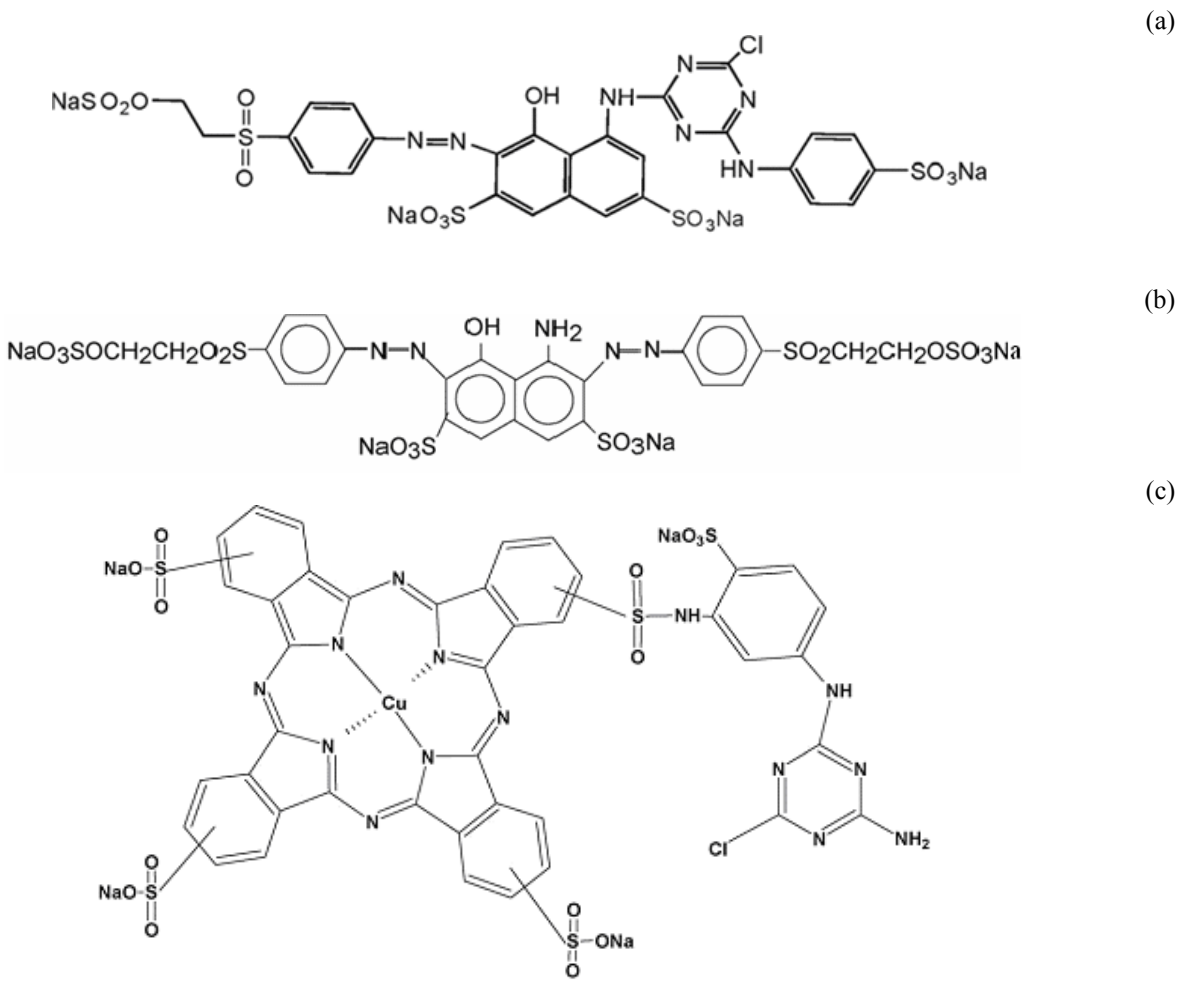

Fig. 1. Molecular structures of RBBA (a), RRR (b) and RTB (c).

necked reactor was designed. Fig. 2 shows the experimental set up used, including: heater, designed reactor and motor stirrer before and after synthesis of Fe_3O_4 NPs (Fig. 2a and 2c). In this set up, nitrogen gas was produced continuously using a nitrogen gas generator (model 2381, Claind, Italy) and was dispersed into the solution through a sparger. The sparger increased degassing efficiency of the solution which protects Fe_3O_4 NPs against critical oxidation by producing very small nitrogen bubbles as is shown in Fig. 2b. For dropwise controlled addition of different solutions such as ferrous and ferric chloride mixer solution, two dropping funnels are connected to the necks of the reactor. Slowly and a dropwise addition of stock solution helps to get high efficiency of the NPs production.

Synthesis of Fe_3O_4 NPs

Fe_3O_4 NPs were prepared by chemical co-precipitation method [30]. First, 10.4 g of $FeCl_3.6H_2O$, 4.0 g of $FeCl_2.4H_2O$ and 1.7 mL of HCl (12 mol L^{-1}) were dissolved in 50 mL of deionized water in a beaker which was degassed with nitrogen gas for 20 min. On the other hand, 500 mL of 1.5 mol L^{-1} NaOH solution was degassed (for 15 min) and heated to 80 °C in the reactor. Then, the stock solution of ferrous and ferric chloride was added dropwise using the dropping funnel during 30 min under nitrogen gas protection and vigorous stirring (1000 rpm) by the glassware stirrer. During the whole process, the solution temperature was maintained at 80 °C and nitrogen gas was purged to prevent the intrusion of oxygen. After the

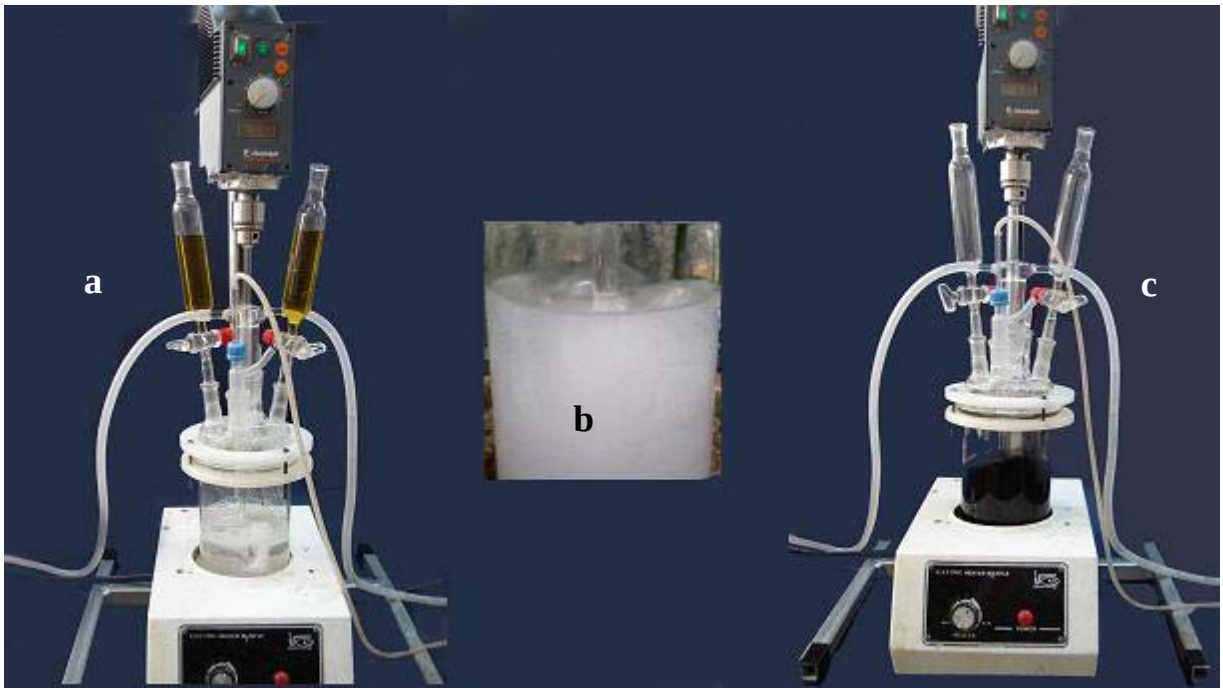

Fig. 2. Image of the set up applied to synthesis of the Fe_3O_4 NPs (a) before addition of ferrous and ferric chloride solution (orange solution in dropping funnel), (b) simultaneous stirring and nitrogen gas bubbling of NaOH solution and (c) after formation of Fe_3O_4 NPs.

reaction, the obtained Fe_3O_4 NPs precipitate was separated from the reaction medium by a magnetic field, and then washed with 500 mL deionized water four times. Finally, the obtained NPs were resuspensioned in 500 mL of degassed deionized water. The pH of suspension after the washings was 11.0 and concentration of the generated NPs in the suspension was estimated to be about 10 mg mL^{-1}. The obtained NPs were stable under these conditions up to one month.

Dye Adsorption Optimization

Optimization studies were carried out according to following procedure: (1) a 40 mL aqueous solution of the dyes (10 mg L^{-1}) were prepared in a 100 mL beakers by the addition of the appropriate amount of the dyes stock solutions, (2) 1.0 mL of the NPs suspension (containing 10 mg of Fe_3O_4 NPs) were added to the dyes solutions, (3) pH of the solutions were adjusted to the desired value and then CTAB was added into the dye solutions, (4) the mixture of the solutions were stirred to enhance the dye adsorption by increasing mass transfer, (5) after dye adsorption; by the use of the strong magnet, CTAB-coated Fe_3O_4 NPs were separated quickly (1 min) from the sample solutions, (6) the residual dye concentrations in the supernatant clear solutions were determined spectrophotometrically using suitable calibration curves. The dye removal steps are shown in Fig. 3 (for RRR as model). The following equation was applied to calculate the dye removal efficiency in the treatment experiments:

$$\text{Dye removal efficiency (\%)} = \frac{(C_0 - C)}{C_0} \times 100 \qquad (1)$$

Where: C_0 and C are the initial and residual concentrations of the dye in the solution (mg L^{-1}), respectively.

Adsorption Isotherm Procedure

Adsorption isotherms were obtained by shaking 12 mg of Fe_3O_4 NPs in 40 mL of the dye solutions (concentrations

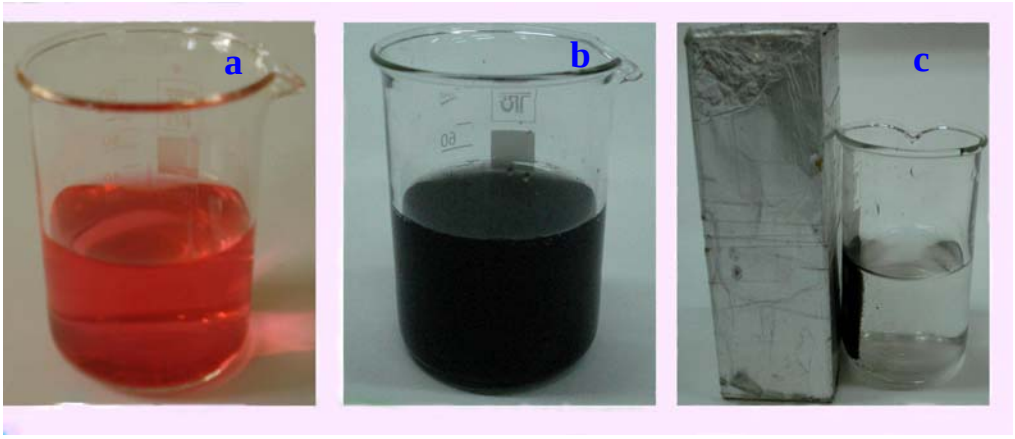

Fig. 3. Images of the dye removal steps: (a) Dye solution before addition of the Fe_3O_4 NPs, (b) dye solution after addition of Fe_3O_4 NPs and the CTAB and (c) Dye solution after being exposed to a very strong magnet.

ranging from 100 to 150 mg L^{-1} for RBBA and RRR, and 100 to 200 mg L^{-1} for RTB) for 12 hrs., under optimum conditions. The solutions were controlled thermostatically at 27 °C by a temperature controlled shaker. The amount of the adsorbed dye on the NPs was calculated based on the following equation:

$$q_e = \frac{V}{W}(C_0 - C_e) \quad (2)$$

Where q_e is the amount of the adsorbed dye on the NPs (mg g^{-1}), C_0 is the initial concentration of the dye (mg L^{-1}), C_e is the equilibrium concentration of the dye in the solution (mg L^{-1}), V is the volume of the dye solution (L) and W is the weight of the used NPs (g).

Also, adsorption of the RBBA, RRR and RTB from simulated wastewaters was studied. The simulated wastewaters contained 60 g L^{-1} Na_2SO_4, 0.1 mmol L^{-1} NaOH, 6 g L^{-1} Na_2CO_3 and 300 mg $L^{-1}$of the dyes was diluted using double distillated water three times and effect of Fe_3O_4 NPs dose and contact time were studied on dye removal.

RESULTS AND DISCUSSION

Characterization of the NPs

Characterization of synthesized Fe_3O_4 NPs was done using IR, XRD and SEM instruments. IR spectra of pure Fe_3O_4 NPs and CTAB-coated Fe_3O_4 NPs is shown in Fig. 4a. The peak at ~ 3455 cm^{-1} is attributed to the stretching vibrations of ─OH, which is assigned to surface OH groups of Fe_3O_4 NPs. The peak at ~ 571 cm^{-1} is attributed to the Fe─O band vibration of Fe_3O_4. Also, the peak at ~ 1380 cm^{-1} is attributed to C─N band and the peaks at 2885 and 2925 cm^{-1} are attributed to two different C─H bands vibration of CTAB. The IR spectra show that Fe_3O_4 NPs surface was well modified by CTAB. Fig. 4b shows the XRD pattern of the synthesized NPs, which is quite identical to pure magnetite (JCPDS No. 07-0322), indicating that the sample has a cubic crystal system. Also, it can be seen that no characteristic peaks of impurities were observed which demonstrates that the designed reactor can be applied to synthesize pure Fe_3O_4 NPs. The SEM image of the prepared NPs is shown in Fig. 4c. Based on the SEM image, the Fe_3O_4 surface morphology analysis demonstrated the agglomeration of many ultrafine particles with a diameter of about 40 nm.

Experimental Design and Data Analysis

Conventional and classical methods of studying a process by maintaining the other factors involved at an unspecified constant level does not depict the combined effect of all the factors involved. This method is also time consuming and requires a number of experiments to determine optimum levels, which are unreliable [33]. Taguchi orthogonal array design (OAD) method is a type of fractional factorial design in which orthogonal array (OA) is used to assign factors to a

(a)

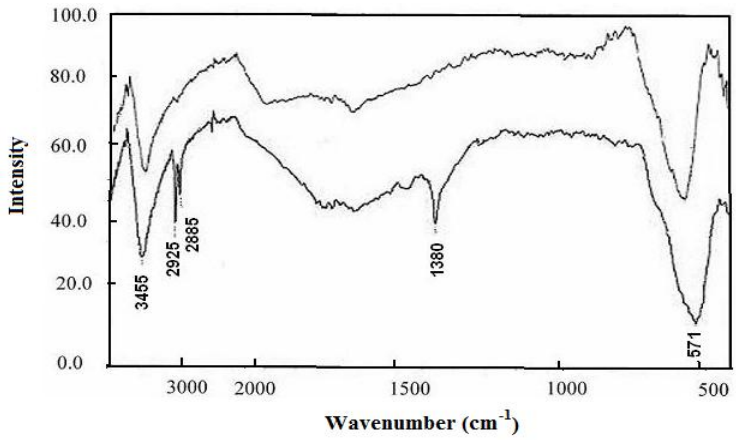

(b)

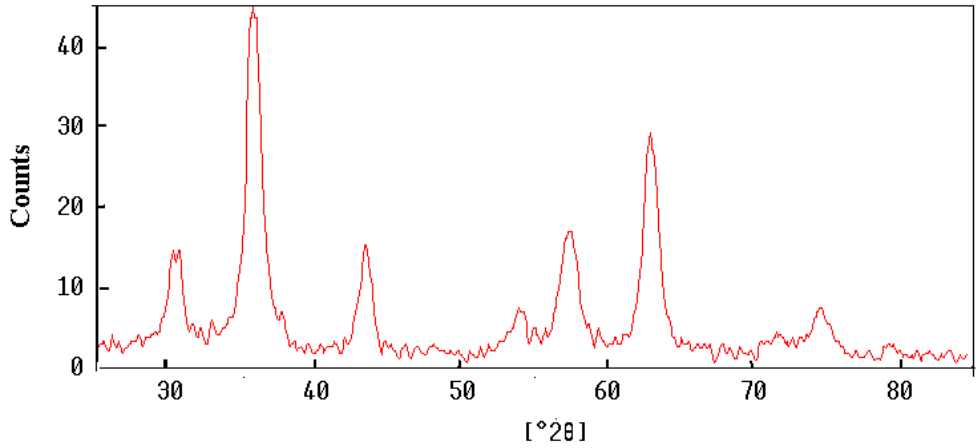

(c)

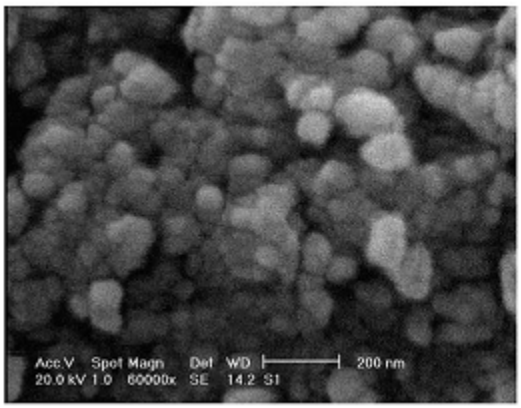

Fig. 4. Characterization of the CTAB-coated Fe_3O_4 NPs.: (a) The IR spectra before and after the modification with the CTAB, (b) The XRD pattern of the Fe_3O_4 NPs and (c) The SEM image of the Fe_3O_4 NPs.

Table 1. Experimental Design Table for the Optimization of RBBA, RRR and RTB Removal Conditions from Aqueous Solutions.

Trial No.	pH	CTAB[a] (mL)	Extraction time (sec)	Salt% (w/v)
1	3	0.0	30	0
2	3	0.2	60	1
3	3	0.6	120	2
4	3	2.0	300	5
5	6	0.0	60	2
6	6	0.2	30	5
7	6	0.6	300	0
8	6	2.0	120	1
9	9	0.0	120	5
10	9	0.2	300	2
11	9	0.6	30	1
12	9	2.0	60	0
13	12	0.0	300	1
14	12	0.2	120	0
15	12	0.6	60	5
16	12	2.0	30	2

[a] Concentration of CTAB is 10 mg mL^{-1}

series of experimental combinations. It can be applied as an experimental design tool, to optimize and evaluate the relative significance of several affecting factors even in the presence of interactions, whose results can then be analyzed using a common mathematical procedure [34]. Equations used to calculate the sum of squares, mean squares, degree of freedom and F-values in the ANOVA method have already been mentioned [35]. A more detailed description of an orthogonal array design was given elsewhere [35].

In this study, a four-factor four-level factorial design (4^4) was used to evaluate the effects of the following factors including pH of the sample solution, the amount of the CTAB, the adsorption time and the NaCl% on the removal of RBBA, RRR and RTB from aqueous solutions. In order to estimate the best conditions for the extraction of the dyes, based on OA_{16} (4^4) matrix, sixteen experiments were done. The factors and their respected levels are reported in Table 1. For increasing the precision of the optimization process each trial was performed twice (n = 32) for RRR and RTB. The percent of the dye removal for the corresponding factors at each level was calculated according to the assignment of the experiment. For example, the removal percent of the four trials at pH = 3 were evaluated as mean values of the corresponding eight runs (each trial has a replicate for RRR and RTB). The mean values of the four levels of each factor (e.g. pH) reveal how the removal percentage will change when changing the level of that factor. Fig. 5 shows removal percentage of the dyes as a function of levels of the studied factors. The ANOVA results for calculated model based on the dyes absorbance are shown in Table 2. The comparison of calculated F values of each factor with their critical values at confidence level of 95% ($P < 0.05$) for RRR and RTB and also at confidence level of 90% ($P < 0.1$) for RBBA was applied to recognize significant parameters (when $F_{calculated} > F_{critical}$ the factor is significant). Also optimum levels of the factors based on the calculated mean effects are listed in Table 2.

Effect of pH

The pH value of the dye solution plays an important role in the whole adsorption process and particularly on the adsorption capacity. Most of the dyes are ionic and upon dissociation confreres dye ions into the solution. The degree of adsorption of these ions onto the adsorbent surface is primarily influenced by the surface charge on the adsorbent, which in turn is influenced by solution's pH [36]. A schematic probable representation of the dye adsorption mechanism is shown in

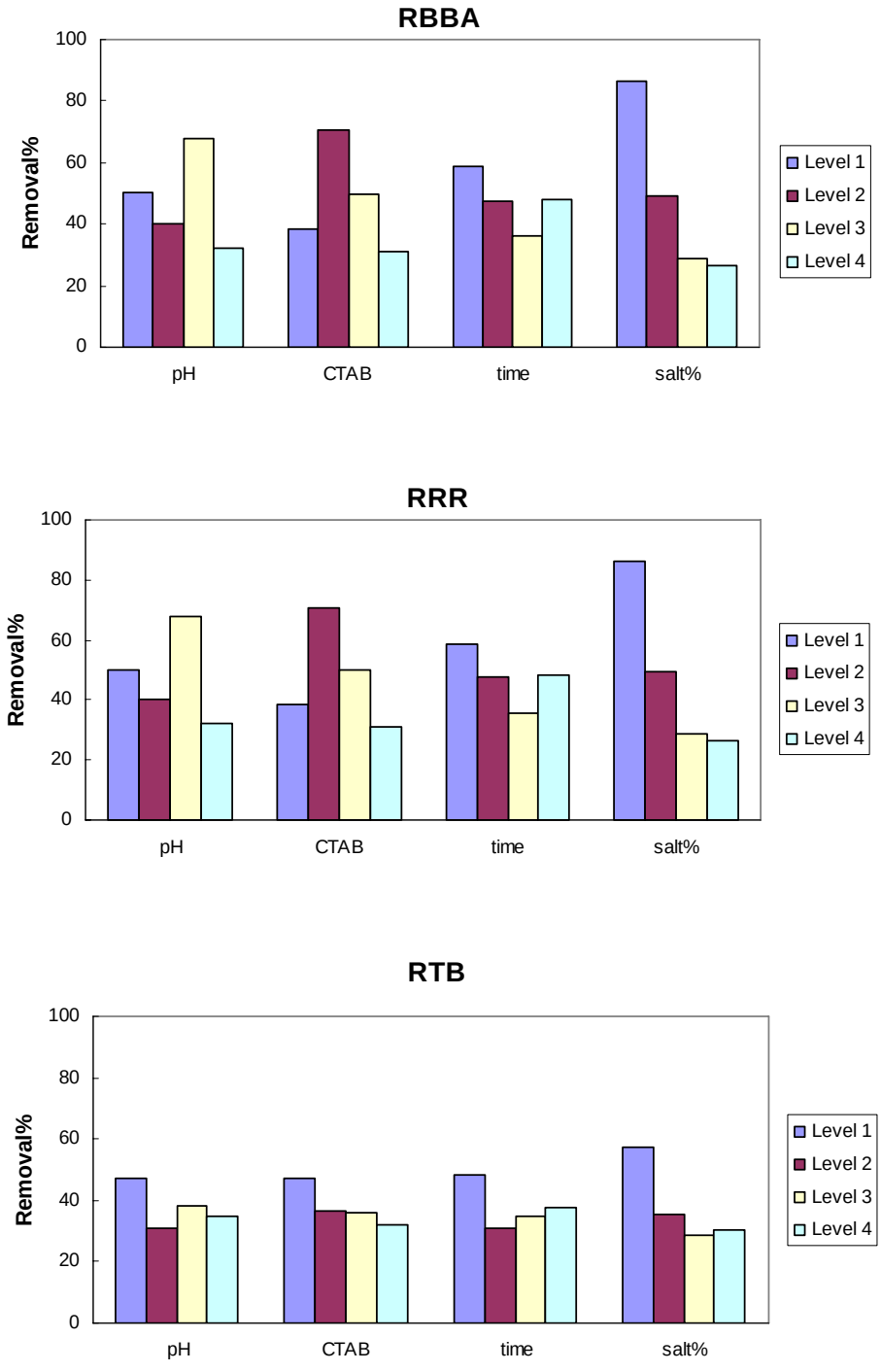

Fig. 5. The effect of the sample solution of the pH, amount of the CTAB: adsorption time and NaCl% of the removal efficiency of RBBA, RRR and RTB from aqueous solutions.

Table 2. ANOVA Table for the Optimization of the Dyes Removal.

Dye	Factor	DOF[a]	Sum of squares	Variance	F-ratio[b]	Pure sum of squares	PC%[c]	Type of effect	Optimum value
RBBA	Sample pH	3	0.003468	0.001156	8.98	0.003082	14.9	significant	9.0
	CTAB amount	3	0.004353	0.001451	11.27	0.003967	19.2	significant	0.2 (mL)
	Removal time	3	0.001278	0.000426	3.31	0.000892	4.3	insignificant	30 (sec)
	NaCl%	3	0.01118	0.003728	28.98	0.010799	54.1	significant	0.0%
	Error	3	0.000386	0.000129			9.3		
	Total	15	0.020669				100.0		
RRR	Sample pH	3	0.008731	0.002910	12.82	0.008050	10.7	significant	9.0
	CTAB amount	3	0.008297	0.002766	12.19	0.007616	10.1	significant	0.0 (mL)
	Removal time	3	0.008896	0.002965	13.07	0.008216	10.9	significant	30 (sec)
	NaCl%	3	0.044947	0.014982	66.03	0.044266	58.8	significant	0.0%
	Error	19	0.004311	0.000227		0.007033	9.4		
	Total	31	0.075181				100.0		
RTB	Sample pH	3	0.048630	0.016210	2.88	0.031732	3.3	insignificant	3.0
	CTAB amount	3	0.492531	0.164177	29.15	0.475632	49.7	significant	0.0 (mL)
	Removal time	3	0.035377	0.011792	2.09	0.018479	1.9	insignificant	120 (sec)
	NaCl%	3	0.272913	0.090971	16.15	0.256015	26.7	significant	0.0%
	Error	19	0.107022	0.005633		0.174614	18.2		
	Total	31	0.956472				100.0		

[a] Degree of freedom

[b] $F_{\text{critical (3, 19; 0.05)}} = 3.13$ and $F_{\text{critical (3, 3; 0.1)}} = 5.39$

[c] Percent contribution

Fig. 6. It seems that both hydrophobic and electrostatic attractions can play role in the adsorption of the dyes.

For Fe_3O_4 NPs, the surface charge is neutral at pH_{zpc}, which is about 7.0 [29]. Based on the ANOVA results (Table 2 and Fig. 5), pH significantly affect RBBA and RRR adsorption efficiency but it is insignificant in the adsorption of RTB. Also, it was found that the maximum adsorption efficiency of RTB and RRR was obtained in an acidic solution of (pH = 3.0). While, the adsorption efficiency of RBBA is maximum at pH = 9.0. These could be attributed to presence of the two different mechanisms in the acidic and alkaline pHs. In the acidic pHs, all of the dyes are in anionic form (due to sulfites groups (Fig. 1)) and can interact with the positively charged surface of Fe_3O_4 NPs. On the other hand, at alkaline pH, surface of Fe_3O_4 NPs is negatively charged and the dyes are negative too. So, the dyes can't directly interact with Fe_3O_4 NPs surface. But in the presence of CTAB, its molecules interact with the negatively charged surface of Fe_3O_4 NPs and create a positive surface at a pH = 9.0 via coating of the surface of Fe_3O_4 NPs (Fig. 6) and then the dyes can interact. The adsorption of the surfactants on the surface of Fe_3O_4 NPs are driven by electrostatic interactions. The obtained results showed that a pH = 3.0 is a favorable pH for adsorption of RRR and RTB, and a pH = 9.0 is the suitable pH for the adsorption of RBBA.

Effect of CTAB

CTAB plays an important role in the dye adsorption mechanism. The ANOVA result shows that the amount of CTAB significantly affects adsorption of the dyes (Table 2). In alkaline conditions like pH = 9.0, the dyes are adsorbed via CTAB on the surface of Fe_3O_4 NPs. Therefore, at alkaline pH, is found with increasing amounts of CTAB, the adsorption efficiency will increase. On the other hand, at high concentrations of CTAB, the adsorption efficiency decreased due to the formation of CTAB (micelles and/or) ion-pairing

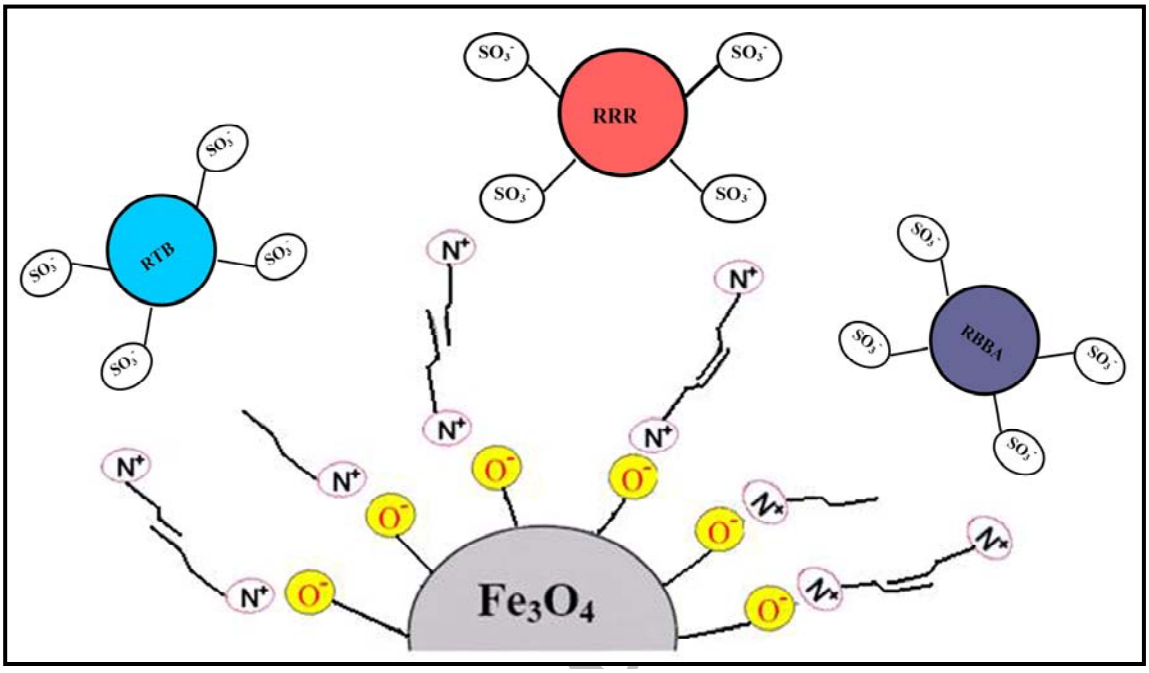

Fig. 6. Schematic illustration of the adsorption mechanism of RBBA, RRR and RTB: on the surface of the CTAB coated-Fe_3O_4 NPs.

between dyes and excess amounts of CTAB which reduce the interaction of negative dyes with positively charged surface of Fe_3O_4 NPs. Under acidic conditions, CTAB can't interact with the positively charged Fe_3O_4 NPs due to electrostatic repulsion. While by increasing the amount of CTAB, it can interact with negatively charged dyes in hydrophobic ion-pairing. So, due to the ion-pairing, electrostatic attraction between positively charged Fe_3O_4 NPs and the negative dyes were decreased, therefore adsorption efficiency also decreased. At very alkaline pHs, there is a competition between OH^- and negatively charged Fe_3O_4 NPs surface to interact with CTAB, therefore adsorption efficiency decreased. Thus, according to the ANOVA results, in subsequent experiments RTB and RRR was extracted in the absence of CTAB, and RBBA was extracted in the presence of 0.2 mL CTAB (10 mg mL^{-1}).

Effect of NaCl Concentration

The effect of salt concentration on the adsorption of RBBA, RRR and RTB (C_{dye} = 10 mg L^{-1}, V = 40 mL) was investigated by the addition of NaCl in the range of 0-5% (w/v). The results are shown in Fig. 5. The ANOVA results showed that as the NaCl concentration increased, the adsorption capacity of the Fe_3O_4 NPs were significantly decreased. Thus, according to Table 2 and Fig. 5, the strategy of no salt addition was selected for the kinetic and isotherm studies.

Effect of Adsorption Time

The NPs have very high surface areas and a short diffusion route, which results in a high extraction capacity and a rapid extraction dynamic. The adsorption time was studied in the range of 30 sec to 5 min. The obtained results (Fig. 5) showed that the adsorption of the dyes was very fast for a 10 mg L^{-1} concentration and reach its equilibrium state within 30 sec for RBBA and RRR, and 2 min for RTB. Such a fast adsorption rates could be related to the absence of an internal diffusion resistance, because adsorption of the dyes occurred only on the surface of Fe_3O_4 NPs.

Table 3. Kinetic Parameters for the Adsorption of RBBA, RRR and RTB on Fe_3O_4 NPs.

Dye	Kinetic model						
	Pseudo-first order		Pseudo-second order			Intra-particle diffusion	
	k_1 (min^{-1})	R_1^2	q_e (mg g^{-1})	k_2 (g mg^{-1} min^{-1})	R_2^2	k_i (mg $g^{-1}min^{-0.5}$)	R_i^2
RRR	47.2	0.7623	108.6	8.5×10^{-3}	0.9998	2.0×10^{-1}	0.8462
RBBA	20.9	0.9225	177.7	3.2×10^{-2}	0.9985	13.1	0.9201
RTB	2.4×10^{-2}	0.9538	161.3	1.9×10^{-1}	0.9999	3.4	0.9268

Adsorption Kinetics

Kinetic parameters, which are helpful for the prediction of the adsorption rate, give important information for designing and modeling the adsorption processes. The removal rate of RBBA, RRR and RTB was very fast during the initial stages of the adsorption processes. However, the equilibrium adsorption times were reached about 15, 45 and 180 min for RTB, RBBA and RRR at 50 mg L^{-1} dye concentration, respectively. The kinetics of RBBA, RRR and RTB adsorptions onto the CTAB-coated Fe_3O_4 NPs were fitted to three conventional kinetic models: pseudo-first order [37], pseudo-second order [38] and intra-particle diffusion [39].

Pseudo-first order: $log\ (q_e - q_t) = log\ q_e - \frac{k_1 t}{2.303}$ (3)

Pseudo-second order: $\frac{t}{q_t} = \frac{1}{k_2 q_e^2} + \left(\frac{1}{q_e}\right) t$ (4)

Intra-particle diffusion: $q_t = k_p t^{0.5}$ (5)

The rate constant and correlation coefficient of each kinetic model are presented in Table 3. It can be seen from Table 3, the correlation coefficient, R^2, for the pseudo-second order kinetic model are much greater than the intra-particle diffusion and first order coefficients for the adsorption of RBBA, RRR and RTB onto the CTAB-coated Fe_3O_4 NPs. These results, strongly confirmed by a chemisorption mechanism which could occur because of electrostatic attraction between negatively charged dyes and positively charged CTAB-coated Fe_3O_4 NPs.

Adsorption Isotherm

The adsorption isotherm is important from both a theoretical and practical point of view. In order to optimize the design of an adsorption system to remove a dye, it is important to establish the most appropriate correlations of the equilibrium data of each system. Equilibrium isotherm equations are used to describe the experimental adsorption data. The parameters obtained from the different models provide important information on the adsorption mechanisms and the surface properties and affinities of the adsorbent. In this study, the two most common isotherms, Langmuir and Freundlich models [40, 41], were used to describe the experimental adsorption data. The linear form of the Langmuir and Freundlich models are written in following equations:

Langmuir model: $\frac{C_e}{q_e} = \frac{1}{K_L q_{max}} + \frac{1}{q_{max}} C_e$ (6)

Freundlich model: $\log q_e = \log K_F + \frac{1}{n} \log C_e$ (7)

The tabulated results in Table 4 suggest that the Langmuir isotherm provides a good model of the adsorption system ($R^2 > 0.999$) for the adsorption of RBBA, RRR and RTB on the CTAB-coated Fe_3O_4 NPs. The maximum monolayer capacities, q_{max}, obtained from Langmuir model are 312.5, 163.9 and 556.2 mg g^{-1} for RBBA, RRR and RTB, respectively. The value of $1/n > 1$ which obtained from Freundlich model indicates that saturation was not attained [42]. So, according to the obtained results, in this system saturation was attained and also the adsorbent surface didn't have heterogeneity.

Desorption and Regeneration Studies

Desorption of the dyes from the adsorbent was studied using different kinds of organic solvents (methanol, acetone, propanol, 50% v/v methanol in HCl, 50% v/v acetone in HCl

Table 4. Langmuir and Freundlich Isotherm Constant for the Adsorption of RBBA, RRR and RTB on Fe_3O_4 NPs.

Dye	Isotherm model					
	Langmuir			Freundlich		
	q_{max} (mg g^{-1})	K_L (L mg^{-1})	R_L^2	n	K_F (L mg^{-1})	R_F^2
RBBA	312.5	1.1	0.9990	14.2	236.6	0.9913
RRR	163.9	0.2	0.9989	4.8	63.9	0.9580
RTB	556.2	2.6	0.9990	11.7	442.9	0.8766

and 50% v/v propanol in HCl (0.1 mol L^{-1})) at 10 mg L^{-1} of RBBA, RRR and RTB. Among the different eluents, desorption ability of methanol was found higher than the other solvents. This can be explained by suitable solubility of CTAB and the dyes in methanol. By using 2 mL methanol, desorption efficiency higher than 99% were obtained in short time (1 min) and only one step elution for RBBA, RRR and RTB. The results showed that Fe_3O_4 NPs can be regenerated by methanol and reused for seven successive removal processes with removal efficiency higher than 99%. Under higher removal cycles, removal efficiency decreasement may be due to oxidation, losing and/or dissolving some amounts of the adsorbent during the successive steps.

Removal of the Dyes from Textile Wastewaters

Under optimum conditions, removal of RBBA, RRR and RTB was studied from the simulated wastewaters. Because of the negative effect of salt and the high salt contents of dyeing wastewaters, the capacity of Fe_3O_4 NPs and its contact time was reconsidered in the simulated wastewaters. The obtained

Table 5. Adsorption Capacities of Different Adsorbents Used for Removal of Reactive Dyes.

Adsorbent	Reactive dye	q_{max} (mg g^{-1})	Ref.
Metal hydroxide sludge	RR-2	62.50	11
	RR-120	48.31	
	RR-141	56.18	
Sorrel's cement	RY-145	107.67	14
	RR-194	120.89	
	RB-B	103.14	
Poly(methylmethacrylate) grafted chitosan	Procion Yellow MX	250	17
	Remazol Brilliant Violet	357	
	Reactive Blue H5G	178	
Modified mesoporous silica	Reactive Yellow GR	92.9	15
	Reactive Red RB	62.4	
Modified bentonite	Reactive Blue 19	206.58	13
Activated carbon developed from orange peel	DB-86	33.78	16
High lime Soma fly ash	Reactive Black 5	7.18	19
Polyacrylic acid-bound iron oxide magnetic nanoparticles	methylene blue	199	
Carboxymethylated chitosan-conjugated Fe_3O_4 NPs	AO12	94.16	20
	AG25	73.53	
CTAB-coated Fe_3O_4 NPs	RRR	163.9	This work
	RBBA	312.5	
	RTB	556.2	

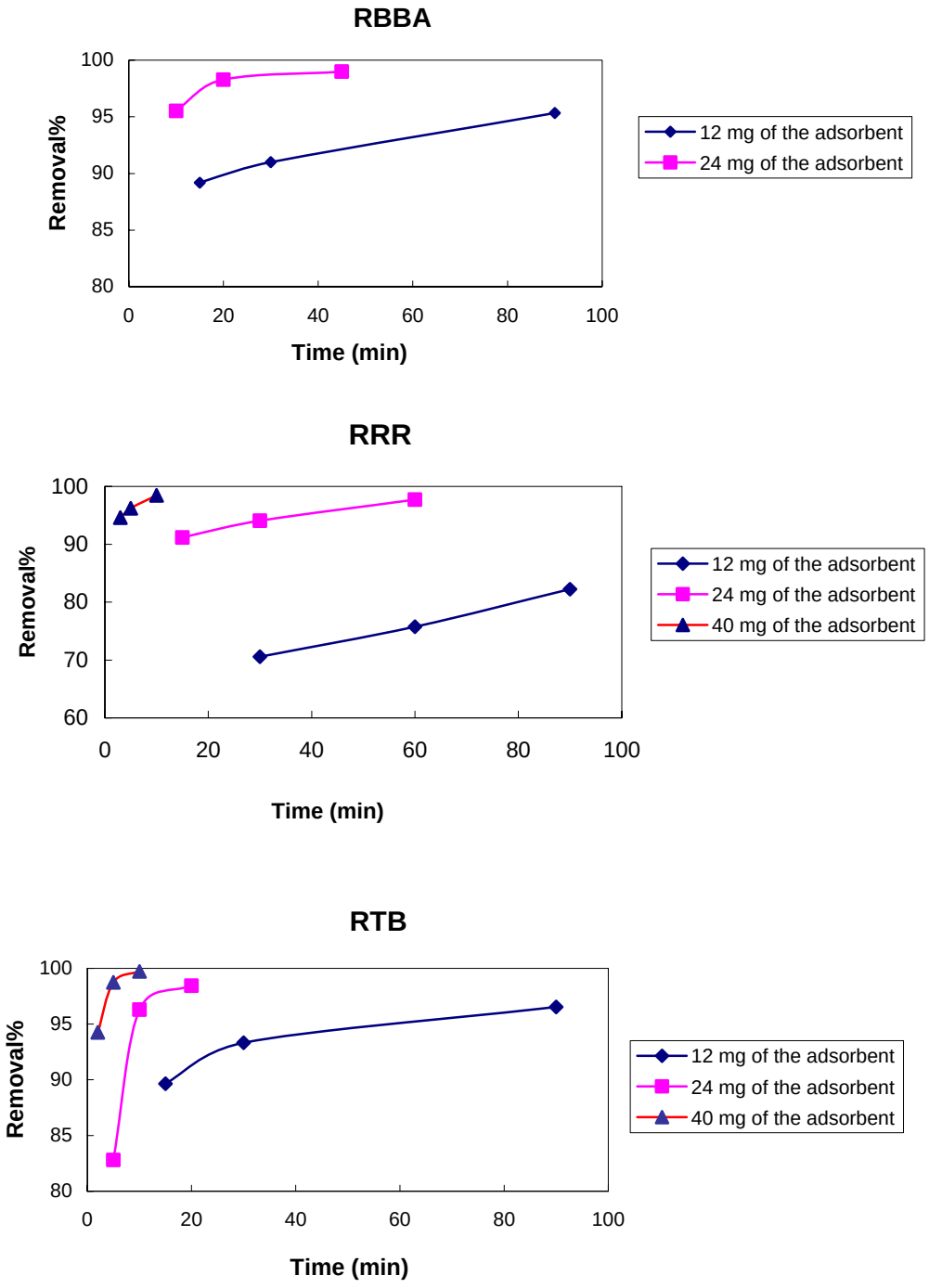

Fig. 7. Removal of the RBBA, RRR and RTB from simulated wastewaters at different Fe_3O_4 NPs amounts and equilibrium times.

results showed that in the presence of high concentrations of NaCl the removal efficiency of RTB and RRR were remarkably decreased. On the other hand, the adsorbent capacity for RBBA was good in the simulated wastewater. According to this observation, removal of RRR and RTB was reconsidered at pH = 9.0 and the addition of 0.2 mL CTAB. The obtained results (Fig. 7) indicate that by applying the new conditions, removal efficiency of RRR and RTB can be remarkably improved. Also, Fig. 7 shows the relationship between the amounts of adsorbent and the required time in order to achieve removal efficiency higher than 90% in the wastewater samples.

CONCLUSION

In the present study, Fe_3O_4 NPs were synthesized by using the reactor and then the CTAB-coated Fe_3O_4 NPs were used as adsorbent for removal of the reactive dyes from wastewater samples. Affecting parameters were optimized using OAD and ANOVA results showed that amounts of CTAB and NaCl significantly affect the removal efficiency of the dyes. Kinetic study showed that kinetic data were well fitted with pseudo-second order model which can confirm by a chemisorption mechanism. Also, experimental adsorption data at equilibrium state were fitted by Langmuir model. Based on the desorption studies, Fe_3O_4 NPs can be regenerated and reused after elution of them by methanol. This study may provide a guideline for efficient removal of other dyes from dye-containing effluents by using magnetic nanoparticles. A comparison on maximum adsorption capacity (q_{max}) of the CTAB-coated Fe_3O_4 NPs for the dyes with other adsorbents which are tabulated in Table 5 reveals its remarkable efficiency over other treated and untreated natural and synthetic adsorbents. Also, Fe_3O_4 NPs as adsorbent can be easily synthesized and regenerated. Due to very high surface areas, short diffusion route and magnetically-assisted separability of the CTAB-coated Fe_3O_4 NPs high adsorption capacities can obtain in a very short time. The reported data should be useful for the design and fabrication of an economically viable treatment process using batch or stirred tank reactors for dye adsorption and for diluting industrial effluents.

REFERENCES

[1] J.J.M. Orfao, A.I.M. Silva, J.C.V. Pereira, S.A. Barata, I.M. Fonseca, P.C.C. Faria, M.F.R. Pereira, J. Colloid Interface Sci. 296 (2006) 480.

[2] J. Weber, V.C. Stickney, Water Res. 27 (1993) 63.

[3] R. Camp, P.E. Sturrock, Water Res. 24 (1990) 1275.

[4] P. Cooper, Color in Dye House Effluent Soc Dyers and Colorists, Alden Press, Oxford, 1995.

[5] L.S. Tsui, W.R. Roy, M.A. Cole, Color. Technol. 119 (2003) 14.

[6] G. Annadurai, R.S. Juang, D.J. Lee, Adv. Environ. Res. 6 (2002) 191.

[7] A. Mittal, J. Hazard. Mater. 128 (2006) 233.

[8] J.F. Osma, V. Saravia, J.L. Toca-Herrera, S.R. Couto, J. Hazard. Mater. 147 (2007) 900.

[9] A. Özcan, E.M. Öncü, A.S. Özcan, Colloids Surf. A: Physicochem. Eng. Aspects 277 (2006) 90.

[10] Y.E. Benkli, M.F. Can, M. Turan, M.S.C. elik, Water Res. 39 (2005) 487.

[11] S.C.R. Santos, V.J.P. Vilar, R.A.R. Boaventura, J. Hazard. Mater. 153 (2008) 999.

[12] F.L. Arbeloa, J.M. Herran Martinez, T.L. Arbeloa, I.L. Arbeloa, Langmuir 14 (1998) 4566.

[13] A. Özcan, C. Ömeroğlu, Y. Erdoğan, A.S. Özcan, J. Hazard. Mater. 140 (2007) 173.

[14] S.S.M. Hassan, N.S. Awwad, A.H.A. Aboterika, J. Hazard. Mater. (In press) 2008.

[15] A.R. Cestari, E.F.S. Vieira, G.S. Vieira, L.P. da Costa , A.M.G. Tavares ,W. Lohb, C. Airoldi, J. Hazard. Mater. 161 (2009) 307.

[16] A. El Nemr, O. Abdelwahab, A. El-Sikaily, A. Khaled, J. Hazard. Mater. 161 (2009) 102.

[17] V. Singh, A.K. Sharma, D.N. Tripathi, R. Sanghi, J. Hazard. Mater. 161 (2009) 955.

[18] V. Rocher, J-M. Siaugue, V. Cabuil, A. Bee, Water Res. 42 (2008) 1290.

[19] S-Y. Mak, D-H. Chen, Dyes and Pigments 61 (2004) 93.

[20] Y-C. Chang, D-H. Chen, Macromol. Biosci. 5 (2005) 254.

[21] A. Henglein, Chem. Rev. 89 (1989) 1861.

[22] H.H. Yang, S.Q. Zhang, X.L.Chen, Z.X. Zhuang, J.G. Xu, X.R.Wang, Anal. Chem. 76 (2004) 1316.
[23] Y. Zhang, N. Kohler, M.Q. Zhang, Biomaterials, 23 (2002) 1553.
[24] H.B. Shen, M. Hu, Y.B. Wang, H.Q. Zhou, Biophys. Chem. 115 (2005) 63.
[25] D. Leun, A.K. Sengupta, Environ. Sci. Technol. 34 (2000) 3276.
[26] M. Faraji, Y. Yamini, M. Rezaee, J. Iran. Chem. Soc. 7 (2010) 1.
[27] Y. Song, S. Zhao, P. Tchounwou , Y-M. Liu, J. Chromatogr. A 1166 (2007) 79.
[28] X.L. Zhao, Y.L. Shi, Y.Q. Cai, S.F. Mou, Environ. Sci. Technol. 42 (2008) 1201.
[29] X. Zhao, Y. Shi, T. Wang, Y. Cai, G. Jiang, J. Chromatogr. A 1188 (2008) 140.
[30] C. Huang, B. Hu, Spectrochimica Acta Part B 63 (2008) 437.
[31] B. Zargar, H. Parham, A. Hatamie, Talanta 77 (2009) 1328.
[32] K.J. Klabunde, Nanoscale Material in Chemistry, Wiley-Interscience, New York, 2001.
[33] K. Ravikumar, S. Ramalingam, S. Krishnan, K. Balu, Dyes Pigments 70 (2006) 18.
[34] Y. Yamini, A. Saleh, M. Khajeh, Sep. Purif. Tecnol. 61 (2008) 109.
[35] R.K. Roy, A Primer on Taguchi Method, Van Nostrand Reinhold, NY, 1990.
[36] K.R. Ramakrishna, T. Viraraghavan, Waste Manage. 17 (1997) 483.
[37] S. Lagergren, Handlingar 24 (1898) 1.
[38] S.H. Chien, W.R. Clayton, Soil Sci. Soc. Am. J. 44 (1980) 265.
[39] W.J. Weber, J.C. Morris, J. Sanity Eng. Div. Am. Soc. Civil Eng. 89 (1963) 31.
[40] I. Langmuir, J. Am. Chem. Soc. 38 (1916) 2221.
[41] H.M.F. Freundlich, Z. Phys. Chem. (Leipzig) 57A (1906) 385.
[42] M.M. Dávila-Jiménez, M.P. Elizalde-González, A.A. Peláez-Cid, Colloids Surface A Physicochem. Eng. Aspect 254 (2005) 107.